Search for a simultaneous signal from small transient events in the Pierre Auger Observatory and the Tupi muon telescopes

C. R. A. Augusto, V. Kopenkin,* C. E. Navia, and K. H. Tsui
Instituto de Física, Universidade Federal Fluminense, 24210-346, Niterói, Rio de Janeiro, Brazil

T. Sinzi
Rikkyo University, Toshima-ku, Tokyo 171, Japan
(Received 12 January 2012; published 2 July 2012)

We present results of a search for a possible signal from small scale solar transient events (such as flares and interplanetary shocks) as well as possible counterparts to gamma-ray burst (GRB) observed simultaneously by the Tupi muon telescope (Niteroi, Brazil, 22.9° S, 43.2° W, 3 m above sea level) and the Pierre Auger Observatory surface detectors (Malargue, Argentina, 69.3° S, 35.3° W, altitude 1400 m). Both cosmic ray experiments are located inside the South Atlantic Anomaly region. Our analysis of several examples shows similarities in the behavior of the counting rate of low energy (above 100 MeV) particles in association with the solar activity (solar flares and interplanetary shocks). We also report an observation by the Tupi experiment of the enhancement of muons at ground level with a significance 8σ in the 1-sec binning counting rate (raw data) in close time coincidence (T-184 sec) with the Swift-BAT GRB110928B (trigger = 504307), according to the GRB Coordinate Network report. At the same time this event was not included in the Swift-XRT products for GRBs. The GRB 110928B coordinates are in the field of view of the vertical Tupi telescope, and the burst was close to the MAXI source J1836-194. The 5-min muon counting rate in the vertical Tupi telescope as well as publicly available data from Auger (15 min averages of the scaler rates) show small peaks above the background fluctuations at the time following the Swift-BAT GRB 110928B trigger. In accordance with the long duration trigger, this signal can possibly suggest a long GRB, with a precursor narrow peak at T-184 sec, or a transient Galactic source.

DOI: 10.1103/PhysRevD.86.022001 PACS numbers: 96.50.S−, 91.25.Rt, 94.20.wq, 95.55.Vj

I. INTRODUCTION

The results of a search for signals from small transient events in association with the muon excess (deficit) registered at ground level (sea level) by the Tupi muon telescopes were reported in 2005 [1,2]. Among the transient events, there were observed signals [in association with the Fermi gamma-ray burst (GBM) spacecraft detector] from the interplanetary shocks as well as solar flares of small scale whose prompt x-ray emission flux is classified as C class (flux smaller than 10^{-5} W m^{-2}) at 1 AU [3].

The high sensitivity attained by the Tupi muon telescopes is a consequence (at least in part) of its physical location within the South Atlantic Anomaly (SAA) region (22.88° S, 43.16° W). According to Stormer's dipole approximation, the geomagnetic rigidity cutoff at the Tupi location is around 8 GV. However, in the SAA the shielding effect of the magnetosphere has a "dip" with an anomalously weak geomagnetic field strength 22 000 nT [4] in the SAA central region 26° S, 53° W), as shown in Fig. 1. The SAA is a result of the eccentric displacement of the magnetic field center of Earth from the geographical center (by about 400 km) as well as the displacement between the magnetic and geographic poles of Earth. The SAA region is clearly indicated by the lowest magnetic field intensity over Earth (Fig. 1); it is limited to the region where the magnetic field strength is less than 28 000 nT, as shown in Fig. 1. The SAA embraces a great part of South America's central region.

Geographical distribution of proton flux measured by the HEPAD ICARE instrument onboard the Argentinean satellite SAC-C [5] shows an excess (up to 10 times) of protons with $E > 850$ MeV in the SAA central region in comparison with the region outside of the SAA (see Fig. 2). It is unlikely that these high energy protons are the Van Allen belt trapped protons because the SAA models such as AP8 [5] and several measurements of the trapped protons showed that their energies do not exceed 300 MeV.

In addition, an analysis on the geomagnetic rigidity cutoff in the SAA area was made by the PAMELA Collaboration [6]. The magnetic rigidity of downward going particles as a function of the geographical latitude was measured with the time of flight system installed in the PAMELA spacecraft. The PAMELA results show that high energy particles are present at all latitudes, while the effect of the low geomagnetic cutoff (below 1.0 GV) on low energy ($E < 200$ MeV) particles is present only at two locations: in the region close to the poles and also in the SAA region. Downward going protons with energies above 200 MeV are also clearly seen at the latitudes between 40° S and 20° S (the SAA area) [6]. These are so-called

*Permanent address: Skobelevskaya st. 42-15, Yuzhnoe Butovo, Moscow, Russia.

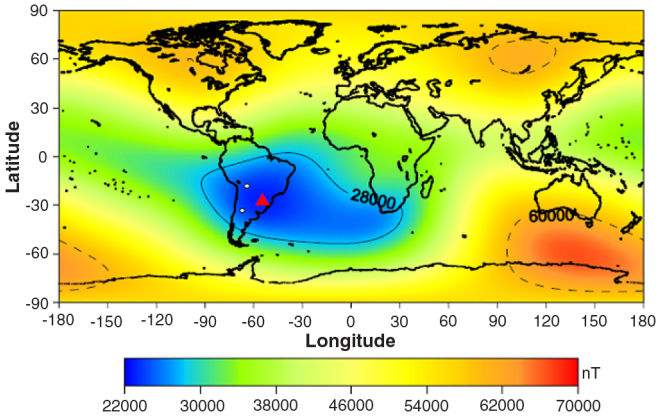

FIG. 1 (color online). Geographic distribution of the geomagnetic field intensity. The SAA boundary is around $B = 28000$ nT. The triangle indicates the SAA central region (Niterói, Brazil, is near this region), where the geomagnetic field intensity is the lowest. The upper circle is the point of Chacaltaya, Bolivia, and the lower point is Auger-Malargüe, Argentina.

"quasitrapped particles." In fact, protons (ions) with energies above 300 MeV in Earth's magnetic field (the SAA area) do not satisfy the Alfvén criterion for particles trapped in the magnetic field. The Alfvén criterion is determined by the following relation: $r_L/r_m \ll 1$, where r_L is the particle Larmor radius and r_m is the curvature radius of Earth's magnetic field line. In short, the PAMELA Collaboration introduced a subcutoff in the rigidity that is below the nominal Stormer rigidity cutoff in the SAA area.

To penetrate to lower altitudes, the solar flare particles must have a rigidity above the cutoff threshold at a given latitude. As the rigidity cutoff decreases, the flux of particles (with the rigidity above the cutoff threshold at a given latitude) increases at a given altitude. The extreme cases are observed in the polar regions and in the SAA region. In these regions the solar flare induced particles will come down to very low altitudes. The solar flares observed by the Tupi telescopes also give support to this conjecture [1,2]. Thus, the shielding effect of the magnetosphere is the lowest in the SAA region. This characteristic permits the observation of small transient events such as solar flares and interplanetary magnetic shocks of diverse origins. In fact, the primary and secondary charged cosmic ray particles can penetrate deep into the atmosphere owing to the low magnetic field intensity over the SAA. Consequently, in the SAA region cosmic ray fluxes at lower energies are even higher than world averages at comparable altitudes. This is reflected as an enhancement in the counting rate of the incoming primary cosmic rays flux.

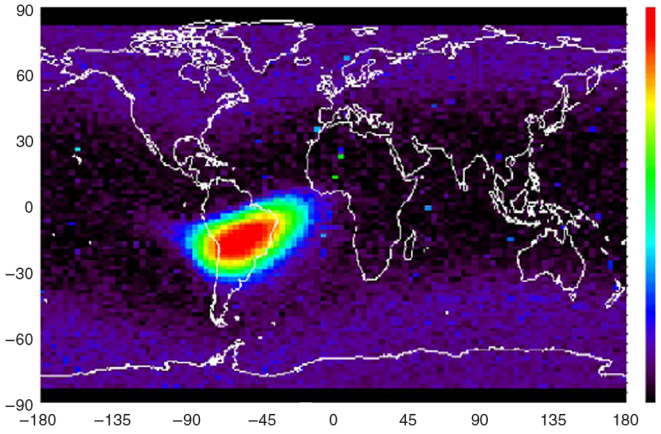

FIG. 2 (color online). Geographical distribution (latitude vs longitude) of proton flux ($E > 850$ MeV) measured by the HEPAD detector [5]. The color scale is logarithmic. The dark color represents 10 times higher proton flux than the one with the light color.

The Pierre Auger Observatory (PAO) was designed to study the physics of cosmic rays at the highest energies. Important results have been already obtained, such as the cosmic ray spectrum [7] and composition in the highest energy region [8]. The PAO is located in Malargüe, Argentina (69.3° W, 35.3° S), 1400 m above sea level and it has a Stormer rigidity cutoff of ~9.5 GV [9]. The temporal variations in the counting rate of low-energy cosmic ray particles (muons and photons) is mainly modulated by the solar activity and properties of interplanetary magnetic field.

In the low energy region ($E > 100$ MeV) the particle flux at ground level is not constant. There are several effects, such as local weather conditions and diurnal solar modulation (so-called "day-night" asymmetry). On the ground the day-night asymmetry is observed as an enhancement in the particle counting rate about 3 hours after sunrise [~12 h universal time (UT)] and up to sunset (~21 h UT) at Tupi and PAO locations. The day-night asymmetry is also subject to seasonal variations. Its origin is explained by the connections between solar and Earth's magnetic fields [10].

We show in this survey that it is possible to identify simultaneous signals from the transient solar events of small scale recorded on the ground by the PAO surface detectors (SD) and the Tupi telescopes. We show here the advantages of observing muons produced by low energy cosmic rays in the SAA region. It is necessary to say a few words about other cosmic ray detectors in the SAA region. It is very well known that neutron monitor signals are used to study low energy solar activity, because neutron monitors are sensitive to even lower cosmic ray energies than a muon telescope. There are two neutron monitors at Mt. Chacaltaya (Bolivia, 5250 m above sea level) located in the region that would allow comparison of experimental data. However, there are no public data available, at least for the time period covered by the present analysis. In general and in most cases previous studies with neutron monitors showed variation in the cosmic particle flux at

ground level in correlation with large scale solar flares classified as X class. For instance, we found the reported ground level enhancement of neutrons in association with solar flares of X class [11] detected by the Chacaltaya neutron monitor.

This paper is organized as follows. In Sec. II a brief description of the PAO SD and the Tupi telescopes is given. The aim is a direct comparison between these two experiments, including such parameters as the energy thresholds and the effective solid angles. The search for the connection among spacecrafts and ground level observations (the PAO SD and the Tupi telescopes) is presented in Secs. III and IV. Section III is devoted to a search for signals associated with the solar flares of small scale, where we derive the energy spectrum of protons accelerated in solar flare, and in Sec. IV we discuss signals associated with the interplanetary magnetic shocks.

Earth's magnetic field deflects the charged particles of air showers. This deflection is caused by the component of Earth's magnetic field perpendicular to the incident particle trajectory. As a result, there is a decrease in the number of collected charged particles that affects the detector efficiency. In the SAA region the magnetic field intensity is low; thus, the capacity of the detectors to respond to incident cosmic ray particles is higher. This behavior is suitable for a search at the ground level of possible signals from GRB. Some results of the search are presented in Sec. V, and the conclusions are drawn in Sec. VI.

II. TUPI TELESCOPES AND THE PIERRE AUGER SD SCALER MODE

The PAO SD [12] is an array of more than 1600 water-Cherenkov detectors placed in a triangular grid with a spacing of 1500 m. The lateral (transverse) distribution of secondary particles of extensive air shower at ground level is sampled by using the SD array, providing a total of about 16 000 m^2 of collection area for the full SD array. The scaler mode consists of recording low threshold rates (scalers) using all the surface detectors of the array. The counter detectors register signals above the threshold value, corresponding to an energy of $\sim$100 MeV deposited by particles that reach the detector. Since September 2005 the typical average scaler rate is around 2000 counts per sec per detector. Details can be found in [13,14].

On the other hand, the Tupi experiment has two muon telescopes [15]. Each telescope was constructed on the basis of two detectors (plastic scintillators 50 cm $\times$ 50 cm $\times$ 3 cm [16–18]) separated by a distance of 3 m. One telescope has a vertical orientation, and the other one is oriented near 45 deg to the vertical (zenith), pointing to the west. Each telescope counts the number of coincident signals in the upper and lower detectors. In addition, the telescope uses a veto or anticoincidence guard system of a third detector close to the two telescopes. This system allows only the detection of muons traveling close to the axis of the telescope. The Tupi telescope is inside a building, under two flagstones of concrete (150 g/cm^2). The flagstones increase the detection muon energy threshold up to $\sim$0.2–0.3 GeV required to penetrate the two flagstones [19]. Time synchronization is essential for correlating event data in the Tupi experiment, and this is achieved by using a global positioning system receiver. Details of the Tupi experiment can be found in [15] and references therein.

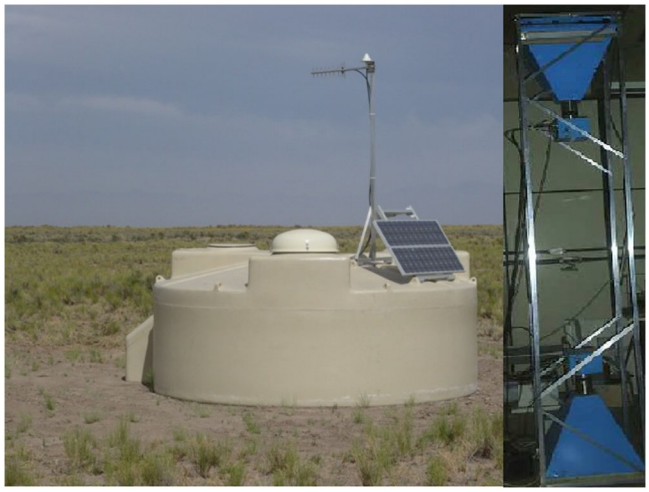

FIG. 3 (color online). View of a unit of the Pierre Auger water-Cherenkov detector (left) and the vertical Tupi telescope (right).

The effective solid angle of each detector (the PAO SD and Tupi) can be roughly obtained from the following relation:

$$\Omega = 2\pi(1 - \cos\theta_z), \tag{1}$$

where θ_z is the maximum zenith angle. For a water-Cherenkov tank detector (the elementary unit of the PAO SD) the effective θ_z is 60°, that gives $\Omega_{\rm eff} = 3.14$ sr. The effective field of view of the Tupi telescopes is estimated as $\Omega_{\rm eff} \sim 0.37$sr, around 8 times smaller than the water-Cherenkov tank detector. This narrow solid angle [20] of the Tupi telescopes is the main difference in comparison with the Cherenkov tank detector solid angle. A photograph of both detectors is shown Fig. 3.

III. SEARCH FOR SOLAR FLARE SIGNALS AT GROUND

The Sun occasionally generates high energy (up to several GeV) particles in association with solar flares. A solar flare occurs as a result of sudden release of the magnetic energy built up in the solar atmosphere. A typical solar flare is accompanied by electromagnetic radiation. The prompt x rays are emitted by electrons accelerated to keV energies in the explosive phase. High energy (MeV–GeV) gamma rays are produced via neutral pion decay as a result of nuclear interactions between solar protons and ions with background nuclei in the flare region [21]. The

electromagnetic emission contains some information on the acceleration mechanism of particles in solar flares [22]. When the solar cycle is at its minimum, active solar regions are small and rare, so only a few solar flares are detected. The number of solar flares increases as the Sun approaches the maximum of its cycle. The period around the solar minimum (quiet conditions of the Sun) is useful for observation of small transient events, such as microflares.

Because of the shielding effect of the geomagnetic field, high energy (MeV–GeV) particles from solar flares can reach only high latitude regions on Earth. The exception to this rule is possible in the SAA region, because of an area of anomalously weak geomagnetic field strength and low rigidity (low subcutoff) to cosmic and solar protons and ions. This feature of the SAA allows observation of small solar transient events such as solar flares of small scale.

However, the detection of solar flares on the ground depends on a combination of several favorable conditions, related to the good magnetic Sun-Earth connection, position of the flare on the Sun disk, and the onset time of the flare. For instance, if the Earth-directed solar flare has been located to the west of the Sun disk at the onset time approximately between (12 h UT) and (23 h UT), then it can be detected by the Tupi-type detector.

On 14 July 2010 the Tupi telescopes registered a muon excess over background 21% in the 5-min binning time profiles (the vertical Tupi telescope). The percent deviation, called "relative variation" R, is defined here as $R = (C^{(i)} - B)/B$, where $C^{(i)}$ is the measured number of counts in the bin "i" and B is the average background count for a given time period. Muon excess is associated with high energy particles emitted by solar flares (protons and ions) with energies above the pion production threshold (because they produce muons in Earth's atmosphere). The flare on 14 July 2010 is a good example of an association with a solar flare of small scale registered by the GOES satellite. The x-ray prompt emission from this solar flare is cataloged by GOES as (C class) [15]. In this survey we found that there is a possible signal associated with this flare in the PAO SD [14]. Figure 4 illustrates the situation. The x-ray flare onset time was determined by GOES as (20:30 UT). This is approximately 1 h before the muon enhancement onset time (21:27 UT) observed by the vertical Tupi telescope and about 1.58 h before the PAO SD small peak at (22:05 UT).

The bottom panel in Fig. 4 shows the time variation of the solar wind temperature as observed by the ACE-SWEPAM satellite detector, located at the Lagrange point L1. It is possible to notice that a signal in this detector is related to the same solar flare. However, the main objective of this bottom panel in Fig. 4 is to show that on 14 July 2010 a small transient event was also observed at (9:00 UT). At this time there was an interplanetary backward shock. A signal from this shock has been registered by both the Tupi telescopes and the PAO SD. Some details of this transient event will be described in the next section.

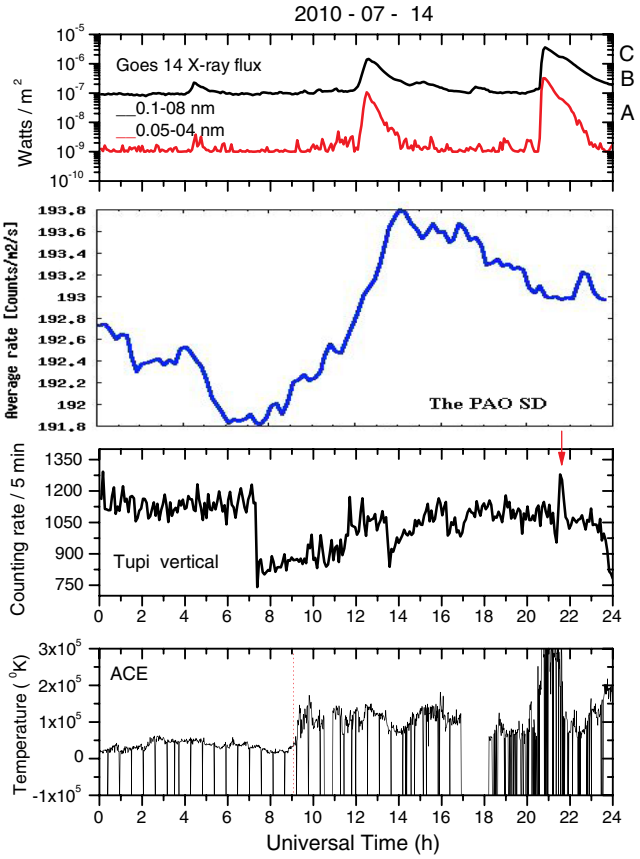

FIG. 4 (color online). Example of a solar flare observation. The x-ray prompt emission of the solar flare at the onset time (20:30 UT) is classified as C class by the GOES14 satellite (top panel). For comparison, there are time profiles of the cosmic ray variation observed by the Earth based experiments: the PAO SD (the second panel from the top, 15 min averages of the scaler rates) and the vertical Tupi muon telescope (the third panel from the top, the 5-min muon counting rate). The bottom panel shows the solar wind temperature observed by the ACE spacecraft located at the Lagrange point L1. The arrow indicates the solar flare signal in the vertical Tupi telescope. Solar flares are classified as A, B, C, M, or X according to the x-ray peak flux (in watts per square meter), as is shown in the top panel.

Another example of small scale solar flare (on 27 May 2011) is shown in Fig. 5. This solar flare was observed on the ground by the Tupi muon telescope. The prompt x-ray emission flux was registered by the GOES satellite at 1 AU. The flare was classified as C2.0 class. The x-ray flare onset time (14:46 UT) determined by GOES is in probable association with a muon enhancement (the signal excess over background $R = 13\%$) observed by the Tupi muon telescope (15:24 UT) (see bottom and middle panels in Fig. 5). This observation by the Tupi telescopes means a plausible quasiprompt emission of high energy solar protons and a coherent nondiffusive particle propagation in the interplanetary solar magnetic field. Again, in association with this small scale C-class flare, there was found a signal in the PAO SD (see top panel in Fig. 5) with the onset time

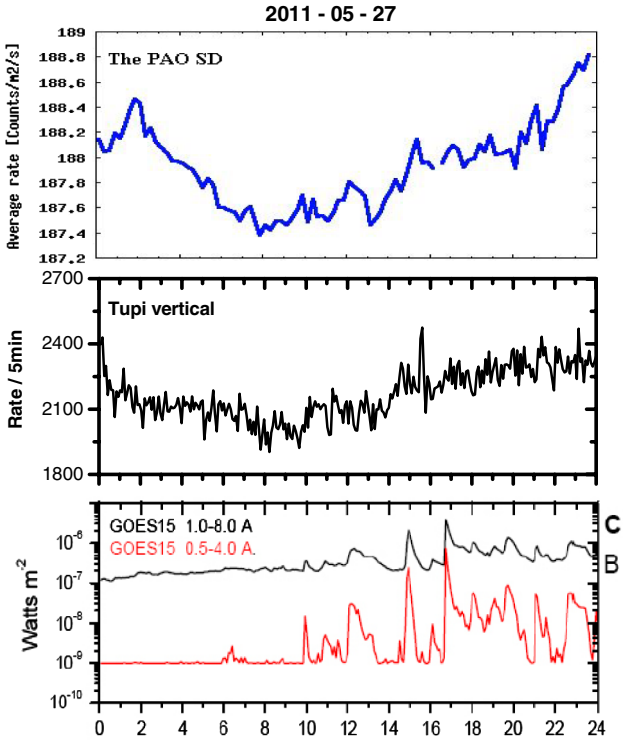

FIG. 5 (color online). A C2.0 class solar flare signal observed at ground as particle counting rate enhancements by the PAO SD with the onset time (15:14 UT) (top panel) and the vertical Tupi muon telescope with the signal excess over background $R = 13\%$ at the onset time (15:24 UT) (central panel). The GOES15 satellite x-ray prompt emission (C2.0 class) was detected at the onset time (14:46 UT) (bottom panel).

(15:14 UT). Thus, we can reinforce the criterion for a quasiprompt association interpretation. We see another coincidence in the position of the signals (peaks) observed by both ground based signals. This is in spite of the fact that the 5-min binning Tupi signal is sharp and narrow in comparison with the PAO SD obtained with the 15 min averages of the scaler rates. One can notice that there is a second flare (C2.3 class) in the data of GOES at the onset time (16:42 UT), but there is no clearly defined signal in either the Tupi telescopes or the PAO SD. In spite of low significance of the signals in the PAO SD, the identification of these two flares (14 July 2010 and 27 May 2011) in the PAO SD data was made possible through a comparison with the Tupi observation as well as data from satellites.

Spectral analysis of the 27 May 2011 solar flare

The minimum proton energy needed to produce pions of energy E_π in the atmosphere is $E_{pth} \sim 10 \times E_\pi$. In the case of the Tupi experiment, the secondary particle energy threshold is $E_s \sim 0.1$ GeV. This means that the minimum proton energy is $E_{pth} \sim 1.0$ GeV. This energy corresponds to a magnetic rigidity of 1 GV.

Cosmic rays (including solar particles) with energy from several dozens of MeV to GeV can reach north and south polar regions, but it is difficult for them to arrive at low or medium latitude regions due to high rigidity cutoff (above ~8 GV). The situation is different near the SAA central region (the Tupi telescope's location) due to the anomalously weak geomagnetic field strength and a subcutoff of around 1 GV. The PAO detector is closer to the border of the SAA region, where the subcutoff is higher and the Stormer geomagnetic rigidity cutoff is estimated as ~9.5 GV.

The specific yield function [23,24], which is the number of muons at sea level per proton, as a function of proton energy near the vertical direction, is determined according to the FLUKA Monte Carlo results [25] and Honda *et al.* [26]. This FLUKA result (see Fig. 6) can be described by the following fitting:

$$S(E_p > 10\ \text{GeV}) = A_{\mu_1} E_p^{\nu_1} \exp(-(E_{0_1}/E_p)^{\lambda_1}), \quad (2)$$

$$S(E_p < 10\ \text{GeV}) = A_{\mu_2} E_p^{\nu_2} \exp(-(E_{0_2}/E_p)^{\lambda_2}), \quad (3)$$

where $A_{\mu_1} = (7.8 \pm 0.60) \times 10^{-3}$, $A_{\mu_2} = (6.8 \pm 0.50) \times 10^{-3}$, $\nu_1 = 1.18 \pm 0.014$, $\nu_2 = 1.18 \pm 0.014$, $E_{0_1} = 10.2 \pm 0.6$ GeV, $E_{0_2} = 10.2 \pm 0.7$ GeV, $\lambda_1 = 1.48 \pm 0.12$, $\lambda_2 = 1.0 \pm 0.0$

The energy spectra of accelerated protons evolve from soft to hard gradually with time. The origin of this behavior is that the charged particles accelerated by solar flare have a power energy spectrum. However, when the energies exceed the threshold of the production of pions, the almost elastic collisions in the atmosphere of the Sun become inelastic, and they lose energy via nuclear interactions (pion production). This transition produces a shift in the spectral index, and the spectrum becomes steeper. Thus,

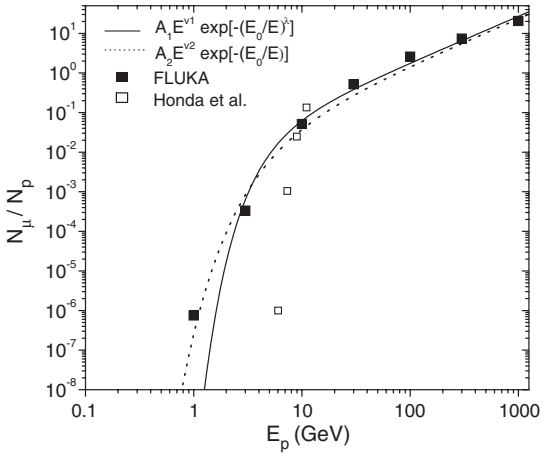

FIG. 6. Yield function, as the number of secondaries at sea level per proton focusing vertically at the top of the atmosphere, as a function of proton energy. The black squares represent the FLUKA Monte Carlo results [25], the open squares are results from [26] for proton energies above 7 GeV, and the lines are two parametrizations used in the present work.

these spectra are in most cases well fit by a double power-law form.

The energy region of our interest, $E_p \geq 1$ GeV, is above the transition region, that is, inside the hard part, with a spectral index ranging from -2.0 to -6.0 [27,28]. The spectral index obtained from observations is an integration over time. There is almost no information on how the energetic particle spectrum changes with time, which introduces some uncertainty in the value of the index. We assumed that the energy spectrum of protons ($E_p \geq 1$ GeV) emitted in solar flares (hard part) is fitted by a single power-law function

$$J(E_p) = A_p\left(\frac{E_p}{\mathrm{GeV}}\right)^{-\beta}. \quad (4)$$

The total number of muons at sea level with energies above E_μ covering an effective area S_{eff}, and in an integrated time T, is a convolution between the yield function and Eq. (4),

$$N_\mu(\geq E_\mu) = S_{\mathrm{eff}} T \int_{E_{p_{\mathrm{min}}}}^{\infty} S(E_p) J(E_p, T) dE_p, \quad (5)$$

since the muon intensity, given by the integral energy spectrum, is

$$I_\mu(>E_\mu) = \frac{N_\mu(\geq E_\mu)}{S_{\mathrm{eff}} T}. \quad (6)$$

The muon's excess allows us to obtain the coefficient, A_p, of the primary proton spectrum as

$$A_p = I_\mu(>E_\mu)\frac{1}{A_\mu}\left(\int_{E_{p_{\mathrm{min}}}}^{\infty} dE_p\left\{\left(\frac{E_p}{\mathrm{GeV}}\right)^{-\beta+\nu} \times \exp\left[-\left(\frac{E_0}{E_p}\right)^{\lambda}\right]\right\}\right)^{-1}. \quad (7)$$

Based on the muon counting rate excess observed by the Tupi vertical telescope on 27 May 2011 in association with the C-class solar flare, the flux is estimated (at 68% C.L.) as $(7.4 \pm 1.6) \times 10^{-2}\ \mathrm{cm^{-2}\,s^{-1}\,sr^{-1}}$ for $\beta = 3$, $(3.4 \pm 0.8) \times 10^{-1}\ \mathrm{cm^{-2}\,s^{-1}\,sr^{-1}}$ for $\beta = 4$, and $(8.4 \pm 1.8) \times 10^{-1}\ \mathrm{cm^{-2}\,s^{-1}\,sr^{-1}}$ for $\beta = 5$, assuming the proton energy threshold 2 GeV.

We estimated the corresponding values for the PAO detector (at 68% C.L.): $(3.0 \pm 0.3) \times 10^{-3}\ \mathrm{cm^{-2}\,s^{-1}\,sr^{-1}}$ for $\beta = 3$, $(6.0 \pm 0.6) \times 10^{-3}\ \mathrm{cm^{-2}\,s^{-1}\,sr^{-1}}$ for $\beta = 4$, and $(7.0 \pm 0.7) \times 10^{-3}\ \mathrm{cm^{-2}\,s^{-1}\,sr^{-1}}$ for $\beta = 5$, where the proton energy threshold is taken as 10 GeV. Figure 7 summarizes the situation. The results of this work are shown by solid squares (the Tupi experiment) for three choices of the spectral index β (5, 4, and 3 from top to bottom) and triangles (the PAO).

Our result (Fig. 7) is compared to other measurements, such as the GOES 8 satellite and the $L3 + C$ underground experiment (threshold ~40 GeV), both for the flare on 14 July 2000 and ground based observation made by IceTop (the energy threshold 0.6 GeV) for the flare on 13 December 2006 [27], and the Baksan underground detector (threshold 500 GeV) for the flare on 29 September 1989 (see [29] and references therein).

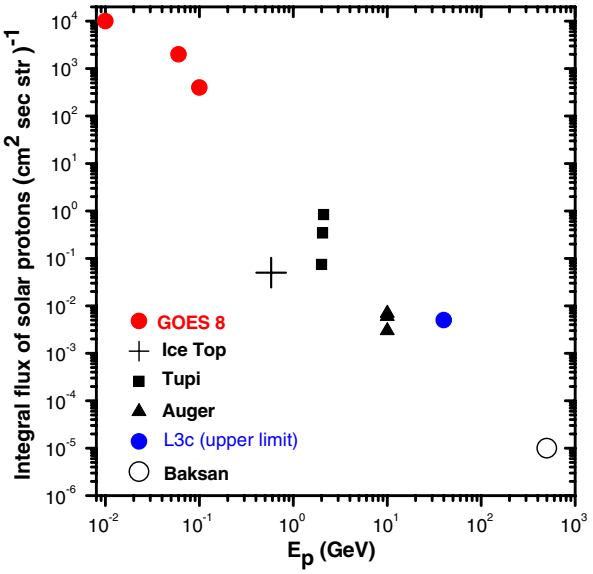

FIG. 7 (color online). The solar flare induced proton flux (integral energy spectrum) obtained by this work for the 27 May 2011 C-class solar flare compared with other measurements [27,29]. See text for details.

IV. SEARCH FOR INTERPLANETARY SHOCK SIGNAL

Usually interplanetary shocks are classified into two classes. The first class of the interplanetary shocks is called coronal mass ejection (CME) [30]. In general, CME can be detected by the Earth based instruments (sensitive to geomagnetic fluctuations) around 2–3 days after the CME explosion. This is the time necessary for the CME ejecta to arrive at the proximities of Earth. If Earth's magnetic field interacts with the solar magnetic field wrapped around the "bubble" of gas from the CME, then a fast fall in the counting rate (shadow effect) in ground detectors (for instance, neutron monitors) is observed. This effect is known as the Forbush event [31]. The magnitude of the Forbush decrease depends on several factors: the size of the CME, the strength of the magnetic fields in the CME, the proximity of the CME to Earth, and the physical location of the detector. The search for muon enhancement at sea level from CME was reported elsewhere [3].

The second class of the interplanetary shocks consists of corotating interaction regions (CIRs) [32]. These are regions of compressed plasma formed at the leading edges of corotating high-speed solar wind streams originated in coronal holes, as they interact with the preceding slow solar wind. The CIRs are particularly prominent features of the solar wind during the declining and minimum phases of the 11-year solar cycle. Figure 8 shows the mechanism

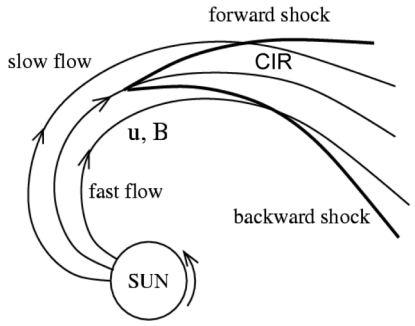

FIG. 8. An illustration of the CIR formation mechanism. The high-speed solar wind, originating in coronal holes, interacts with the preceding slow solar wind forming forward and reverse shocks. Marks are u, speed of the solar wind, and B, magnetic field strength.

of CIR formation, where the forward shock and reverse shock are the regions where particles of interplanetary space are accelerated.

The registration of shock waves on the ground in association with the spacecraft detectors located at the Lagrange point L1 allows us to determine whether the shock was propagating forward or backward (in relation to the Sun). The forward shock configuration happens if the CIR is formed at a distance less than 1 AU, particularly when the CIR spread is close to the Sun-Earth direction. In this case, at first the shock reaches the Lagrange point L1 and some time later it arrives at Earth.

On the other hand, registration on the ground of backward shock waves (directed away from the Sun) is possible if the CIR is formed at a distance above 1 AU. In this configuration, at first the shock reaches Earth and then the Lagrange point L1. Depending on the shock speed, a time delay of the shock (for about 1–2 h) between the observation of the shock at the Lagrange point L1 and Earth, or vice versa, can be expected.

An example of a CIR observed at the distance of 1 AU on 14 July 2010 at (7:15 UT) as a fall in the Tupi muon counting rate is shown in Fig. 4 (see the previous section). In this interpretation, the shock wave crossed Earth at first, and then, about 1.6 h later (see vertical lines) it reached the spacecraft ACE position, that is located at the Lagrange point L1. An increase in the temperature of the solar wind (see Fig. 4) is observed. Consequently, this shock can be classified as a reverse shock. A clear association between the Tupi signal (a fall in the counting rate with the signal $R = 37\%$ excess over background) and the ACE satellite solar wind temperature is observed. A signal is also found in the PAO SD. This signal appears as a fall in the counting rate ($R \sim 18\%$) with the onset time $\sim$1 h in relation to Tupi.

On 29 March 2011, according to the ACE and SOHO solar detectors, there was an interplanetary forward shock with the onset time (15:00 UT) with a confidence level of 68%. The effect of this shock was detected by ground

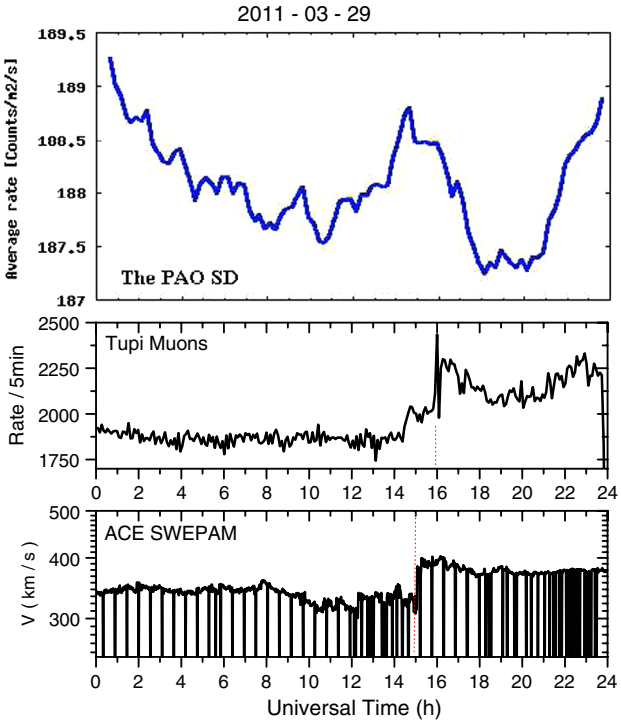

FIG. 9 (color online). Example of a forward interplanetary shock (CIR) observed at 1 AU as a fast rising in the muon counting rate registered by the inclined Tupi telescope on 29 March 2011 (central panel). The signal observed by the PAO SD is shown in the top panel. The solar wind speed observed by the ACE spacecraft at Lagrange point L1 is presented in the bottom panel. The vertical lines indicate the CIR onset time determined by Tupi and ACE. A sudden increase followed by a fall in the counting rate (shadow effect) can be seen in the ground based data.

detector (the Tupi muon telescope) as a sudden increase followed by a fall in the counting rate (shadow effect). There is $\sim$1 h time delay between the onset time determined by the satellites and the Tupi telescopes. The counting rate variation in the Tupi telescope has $R \sim 10\%$. A signal is also observed in the PAO SD. There is a fall in the counting rate with the signal excess over background near 1%, as can be seen in Fig. 9.

V. SEARCH FOR GAMMA-RAY BURST SIGNALS AT GROUND

Gamma-ray bursts (GRBs) are probably the most powerful explosions observed in the Universe today. The total energy released is typically of the order 10^{51} erg. The origin and production mechanism of GRBs is not yet very well understood. However, there are some evidences that they are probably generated by collapsing massive stars (for long GRBs) and merging of two neutron stars (for short GRBs) [33–35]. Some long GRBs are usually followed by emission of all sorts of radiation from radio waves to GeV photons. The GRB sources are randomly

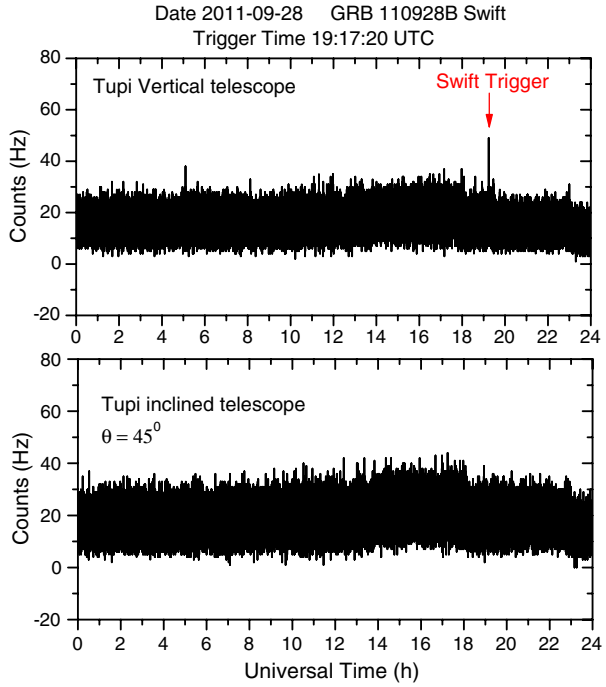

FIG. 10 (color online). Time profile of the 1-sec binning counting rate (raw data) observed by the vertical (top panel) and inclined (bottom panel) Tupi telescopes on 28 September 2011. The vertical arrow indicates the Swift-BAT GRB 110928B trigger.

distributed over the whole sky, and the GRBs are observed by satellite based detectors at a rate as much as 2–3 bursts per day. Information from GRBs by the satellite gamma-ray detectors are distributed to ground based detectors via the GRB Coordinate Network (GCN) [36]. The main parameters are the GRB trigger time and the GRB trigger coordinates. They are essential for a search of counterparts to GRB at ground (GeV component as well as afterglow). In March 2005 the scaler mode was implemented in all the detectors of the PAO SD [37], in order to search for GRBs. It was also included in the LAGO project [38], a network of water-Cherenkov detectors at high mountain altitudes. So far, no positive results have been reported by either of these detectors.

However, the Tupi observations have produced some experimental evidences for a delayed signal in relation to the Swift GRB 080723 and Fermi GBM 081017474 [39]. In addition, the event Konus GRB090315 (Hurley *et al.*, GCN Circular 2009 [40]) and the Swift GRB091112 [41] have probable correlations with the observed muon excess.

On 28 September 2011, a sharp peak with $N_{\max} = 49$ counts was found at (19:14:61 UT). It was possible to recognize this peak in the time profile of the muon excess just with the naked eye (see Fig. 10). The signal was absent in the inclined Tupi telescope. The peak with a duration of 1 s has been registered in close temporal coincidence

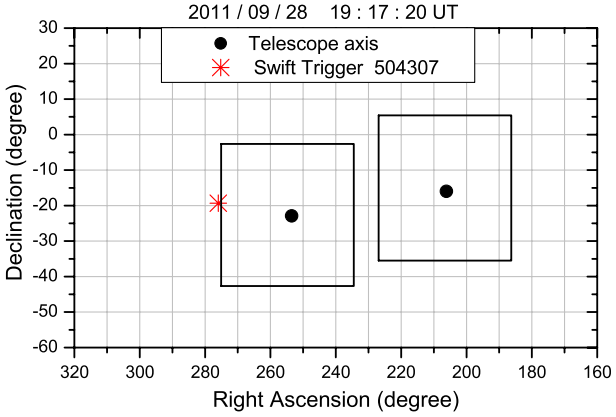

FIG. 11 (color online). The equatorial coordinates of the Tupi telescope's (vertical, on the left, and inclined, on the right) axes (black circles). Squares represent the field of view of the telescopes and the asterisk is the position (coordinates) of the Swift-BAT GRB110928 (trigger = 504307).

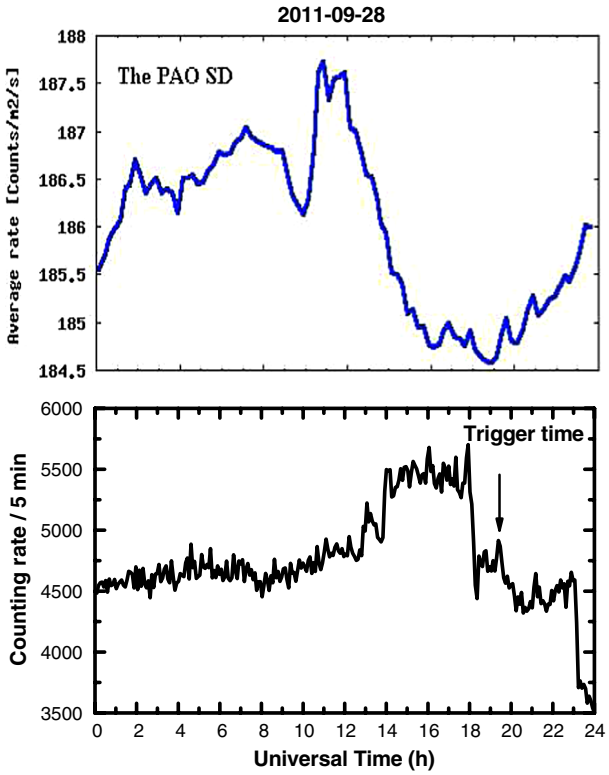

FIG. 12 (color online). Comparison between the time profiles observed on 28 September 2011 by the PAO SD (top panel) in the 15-min averages data and the 5-min muon counting rate in the vertical Tupi telescope (bottom panel) on 28 September 2011. The vertical arrow indicates the time of the Swift-BAT GRB 110928B trigger.

(T-184 sec) with the Swift-BAT GRB110928B (trigger = 504307). The Swift-BAT trigger at (19:17:20 UT) had a long duration of 17.1 min, and the image significance was determined to be 7.79σ [42]. Figure 10 summarizes the

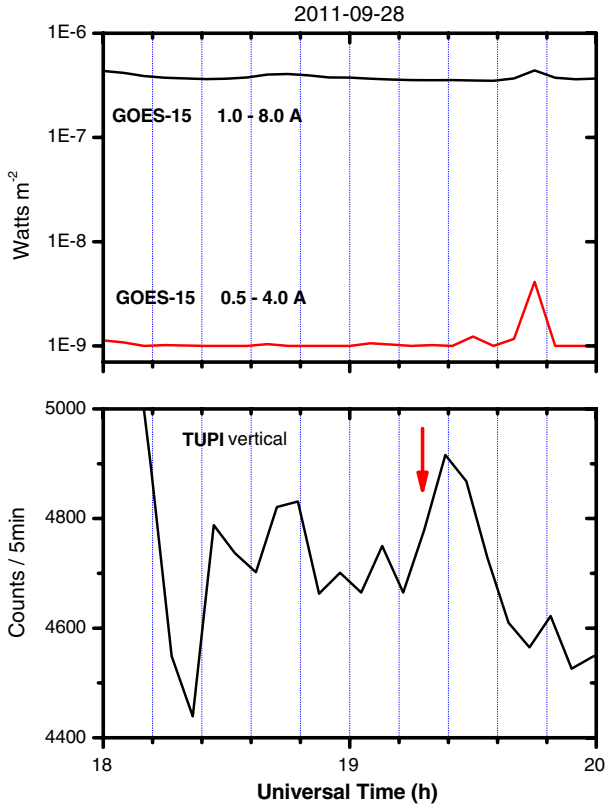

FIG. 13 (color online). Top panel: The x-ray flux on 28 September 2011, according to GOES 15, for two wavelengths. Bottom panel: The 5-min muon counting rate in the vertical Tupi telescope. The vertical arrow indicates the time of the Swift-BAT GRB 110928B (trigger = 504307).

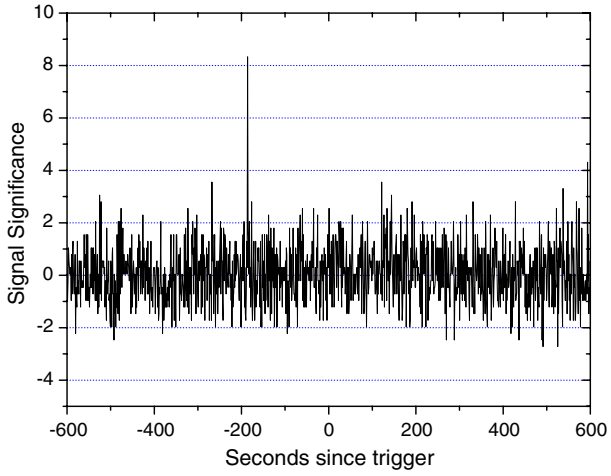

FIG. 14 (color online). Signal significance at the 1-sec binning counting rate observed by the vertical Tupi telescope as a function of time elapsed since the Swift-BAT GRB110928 trigger time. Here the time period is 1200 s ± 600 s around the trigger.

situation, where the time profiles of the vertical and inclined Tupi telescopes on 28 September 2011 are shown. It was reported that the Swift-BAT GRB110928B at the position of $(RA, Dec) = (278.950, -19.328; J2000)$ [42]

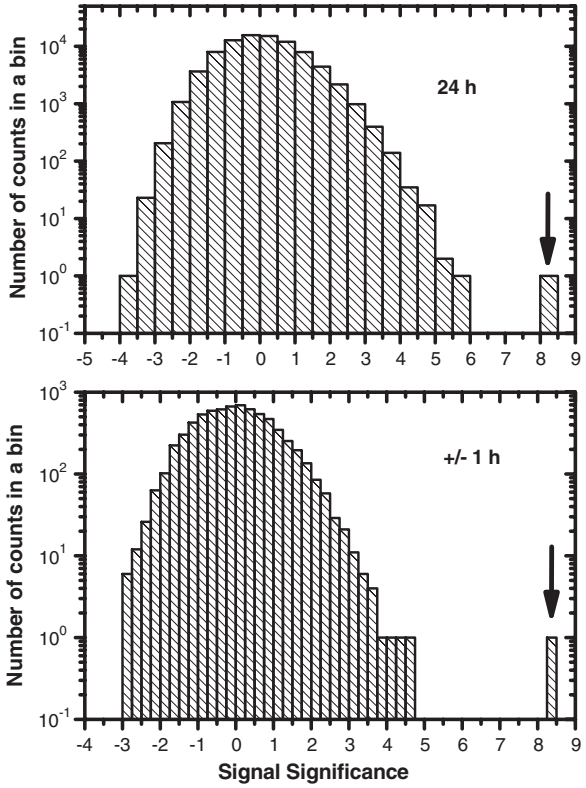

FIG. 15. Distribution of the signal significance in the vertical Tupi telescope. Top panel: A period 24 h (28 September 2011). Bottom panel: period of 1 h around the Swift-BAT GRB110928 trigger. An arrow indicates the signal significance for the Tupi 28 September 2011 event.

corresponds to the MAXI source J1836-194, lying only 70 arcsec away [42], where "MAXI" stands for a sensitive x-ray slit camera attached on the Japanese Experiment Module (JEM) Kibo at the International Space Station. It is interesting that the MAXI J1836-194 is the newly discovered (on 2011 August 30) transient source at the position of $(RA, Dec) = (279.12, -19.41; J2000)$ in the Sagittarius constellation [43]. It was also reported as a black hole candidate x-ray binary [44]. It is necessary to stress that the trigger coordinates are in the limit of the effective field of view of the vertical Tupi telescope (as can be seen in Fig. 11).

We searched for a possible simultaneous signal in the PAO SD as well. The 5-min muon counting rate in the vertical Tupi telescope as well as publicly available data from the PAO SD (15 min averages of the scaler rates) show small simultaneous peaks above the background fluctuations at the time following the Swift-BAT GRB 110928B trigger. If confirmed, this signal could possibly reinforce the GRB interpretation, as shown in Fig. 12.

In addition to that, there were found no flare or transient events (see Fig. 13), as well as no anomalous changes in

the atmospheric pressure, temperature, or other known environmental conditions during the time period close to the signal detection on 28 September 2011. One can notice that the width of the peak at half of the height (near the Swift trigger) is close to the trigger duration (see Fig. 13).

Evidently, a more robust analysis in the original PAO SD is necessary, in order to confirm whether this small signal is really a true signal or just a mere coincidence with some background fluctuation [45]. As we do not have access to the PAO SD raw data, the fine analysis was made only on Tupi data.

VI. ANALYSIS OF THE TUPI 28 SEPTEMBER 2011 EVENT

A. Signal and background

A minimum live time interval in the Tupi telescope is 1 sec. The exact bin size is defined by the Tupi telescope data acquisition system. The vertical Tupi telescope has been tested by bin selection criteria (BSC). According to this algorithm, the signal significance S in the ith bin is defined as

$$S_i = \frac{(C^{(i)} - B)}{\sqrt{B}}, \tag{8}$$

where $C^{(i)}$ is the measured number of counts in the bin "i" and B is the average background count for a given time period. This function follows a Gaussian distribution if there is no signal. The result of the BSC analysis for ± 600 s around the trigger time is shown in Fig. 14.

We have also chosen the intervals 24 h and 1 h around the Swift-BAT GRB110928 trigger time in Fig. 15. Again, the distribution of the muon counting rate in the vertical telescope is consistent with a Gaussian distribution. For a 24 h period the signal significance is $49 - 15.84/\sqrt{15.84} = 8.33$, where the 24 h average background count is $N_{bg} = 15.84$ with the standard deviation 4.27. The signal in the vertical Tupi telescope has a significance above 8σ. No similar excess of the muon flux was observed in this day.

Thus, we can see an excess over the background. We estimate the probability that the excess is due to background fluctuation. The total number of trials is equal to the number of bins N_{bin} during the considered time interval. The probability of random realization of this excess due to background fluctuations in any of 1 s bins during the given time period (24 h) at the day of the burst can be expressed as $P = 1 - \exp(-N_{bin} \times q)$, where q is Poisson probability of the burst with amplitude $N_{\max}$ in the time

TABLE I. Basic information on GRBs observed in the field of view of the vertical Tupi telescope. The Tupi experimental data are for the period July 2010–November 2011. Δt stands for the time elapsed since the trigger and is based on the Tupi experimental data. $N_{\max}$ shows maximum number of counts in 1 s bin during interval 1000 s ($\pm$ 500 s around the trigger). The signal significance S is calculated using the BSC method.

N	Date (yy/mm/dd)	Time (UT)	(Ra;Dec)	GRB/Trigger	Δt	$N_{\max}$	S
1	2010/08/15	22:40:09.910	(244.131; −13.827)	Swift (431762)	−488	25	3.6
2	2010/08/26	22:58:22.898	(284.000; − 23.190)	Fermi (bn100826957)[a]	+253	27	4.6
3	2010/09/10	19:37:43.963	(238.100; − 34.620)	Fermi (bn100910818)[b]	−8	25	3.0
4	2010/10/21	00:13:25.356	(0.867; − 23.710)	Fermi (bn101021009)[b]	+53	23	3.2
5	2010/11/02	20:10:07.430	(284.679; − 37.030)	Fermi (bn101102840)	−134	29	5.0
6	2010/11/26	04:44:27.477	(84.771; − 22.550)	Fermi (bn101126198)[b]	−112	29	3.0
7	2010/11/27	02:27:30.903	(70.950; − 11.320)	Fermi (bn101127102)	−233	28	3.2
8	2010/11/28	07:44:04.238	(145.471; − 35.200)	Fermi (bn101128322)	−145	27	2.9
9	2010/12/19	02:31:29.520	(74.616; − 2.534)	Swift (440606)[b,c]	−396	30	4.0
10	2011/03/18	13:14:19.600	(338.274; − 15.282)	Swift (449542)[d]	−309	25	4.0
11	2011/04/09	04:17:20.600	(238.7; − 34.32)	Fermi (bn110409179)	+411	22	3.8
12	2011/05/26	17:09:01.809	(102.479; − 16.420)	Fermi (bn110526715)	+94	21	4.4
13	2011/06/18	18:14:16.307	(147.050; − 7.480)	Fermi (bn110618760)	−127	26	3.2
14	2011/07/17	04:19:50.66	(308.467; − 7.850)	Fermi (bn110717180)[b]	−298	21	3.6
15	2011/07/21	04:47:43.761	(332.454; − 36.628)	Fermi (bn110721200)[b]	−43	23	4.3
16	2011/07/30	00:11:54.743	(263.079; − 22.780)	Fermi (bn110730008)	−371	23	3.8
17	2011/08/29	23:41:12.040	(278.721; − 8.751)	Swift (501752)	+151	33	3.4
18	2011/09/09	02:46:58.190	(347.342; − 24.220)	Fermi (bn110909116)[e]	−495	26	3.7
19	2011/09/28	19:17:20.580	(278.950; − 19.328)	Swift (504307)	−184	49	8.2

[a]Also observed by Konus-Wind at (22:58:29.729 UT) [50].
[b]Also observed by Konus-Wind [50].
[c]The observed energy spectrum for this GRB ($z = 0.718$) is available in [51]. No spectra are available for other GRBs in the list.
[d]Also observed by Fermi (trigger 322146858/bn110318552) [52].
[e]Also observed by Konus-Wind at (02:47:02.530 UT) [50].

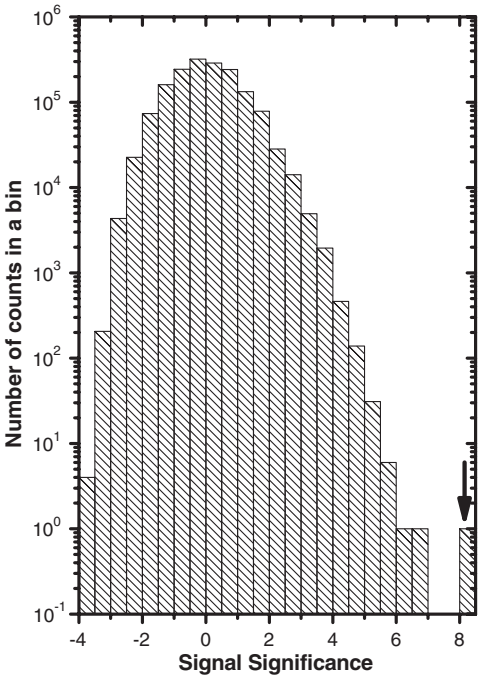

FIG. 16. Distribution of the signal significance in the vertical Tupi telescope as a result of superposition of 19 days from the period July 2010–November 2011 (see Table I). During this period the satellites detected 19 GRBs that occurred in the field of view of the vertical Tupi telescope. An arrow indicates the signal significance for the Tupi 28 September 2011 event.

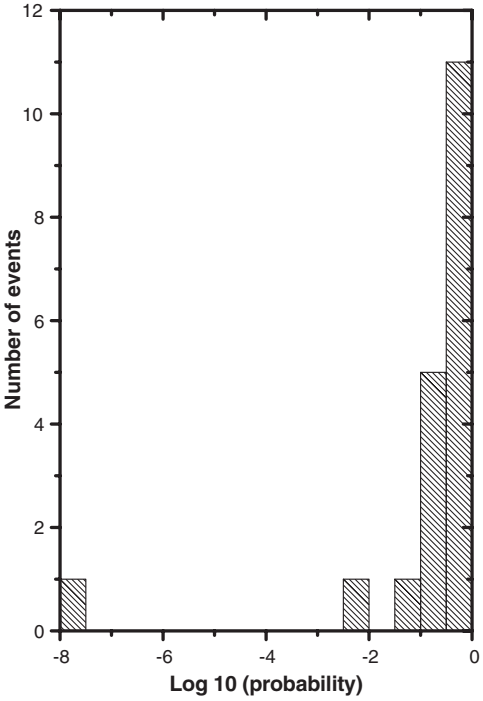

FIG. 17. Distribution of probabilities (in the logarithmic scale) that the observed excess for the 19 GRBs is due to fluctuations in the 24 h background during a ± 500 s period around the trigger time.

interval with the given background N_{bg} (for 24 h). We found that the probability for such an excess being due to a background fluctuation is $\sim 1.15 \times 10^{-6}$ for 24 h.

B. Search for other GRBs in the field of view of the vertical Tupi telescope

Following this analysis, we checked whether there were other possible excesses in the vertical Tupi telescope corresponding to the GRB trigger time reported by the satellites. We found that in the operational time period [46] from January 2010 until November 2011 there were 19 GRB trigger candidates detected by the Swift and Fermi satellites in the field of view of the vertical Tupi telescope. Table I lists basic information on these GRBs. The experimental data on counting rate of muons in the vertical Tupi telescope were checked for possible excesses ± 500 s around the trigger time of each GRB reported by the satellites. The maximum number of counts during a 1000 s period ($\pm$ 500 s around the trigger) is taken as a signal, and the average number of counts during 24 h is taken as a background. For each burst, we define three experimental parameters in this analysis: the maximum number of counts in a bin, the signal significance, and the difference between the observed signal and the trigger.

Distribution of the signal significance in the vertical Tupi telescope based on superposition of 19 days is presented in Fig. 16. We can see again that the 28 September 2011 event stands out from the rest of the sample.

Figure 17 presents the distribution of probabilities for 19 GRBs, plotted on a log-linear scale, with logarithmic scale for the x axis. This figure illustrates the significance of the excess for the Tupi 28 September 2011 event. It can be seen that the other 18 GRBs are compatible with the fluctuations in the background during a ± 500 s period around the trigger time.

In the present analysis we noticed that the distribution of time elapsed since the trigger (see Table I) in the period ± 500 s around the GRB trigger shows some excess for the precursor events, as can be seen in Fig. 18. We believe that further experimental observations are necessary in order to get better statistical constraints for this observation.

C. Spectral analysis of the Tupi 28 September 2011 event

While the signal in the vertical Tupi telescope seems to be a good candidate for the counterpart associated with the GRB110928B, some numerical estimations are necessary in order to consider this interpretation. In order to produce muons, the GRB energy spectrum must extend beyond the GeV region (energy threshold to produce muons). Let us assume that the Tupi 28 September 2011 event is originated by a high energy gamma ray producing muons in the atmosphere. Unfortunately, the satellite based energy

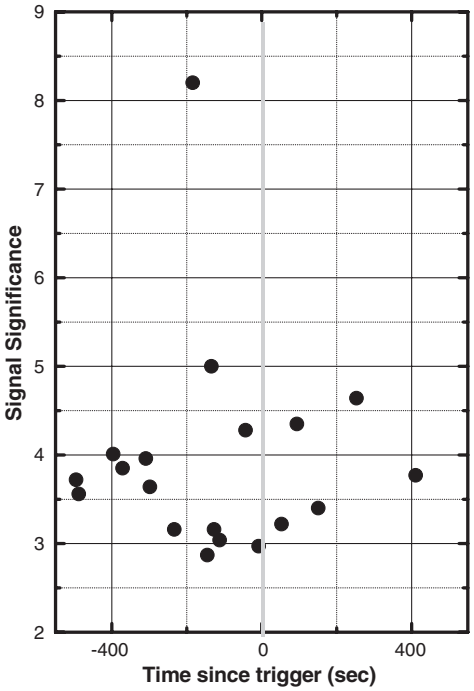

FIG. 18. Correlation between time elapsed since the GRB trigger and the signal significance in the interval ±500 s around the trigger. The elapsed time is based on the Tupi experimental data on muon counting rate.

spectrum and maximum energy of emission were not available for the GRB110928B. To estimate the primary energy of gamma rays which could be at the origin of the observed excess, here we use a method that is similar to the one presented in Sec. III that is based on Monte Carlo simulation using the simulation code FLUKA. The FLUKA Monte Carlo [47] takes into account the photon charged-particle conversion in the atmosphere. In the present case the FLUKA yield function represents the number of charged particles near the vertical direction at sea level per photon as a function of photon energy (see Fig. 19).

The FLUKA results can be described by the following fitting equation:

$$S(E_\gamma > 10\ \text{GeV}) = A_\mu E_\gamma^\nu. \tag{9}$$

It can be seen from Fig. 19 that the effective energy threshold for production of secondary charged particles at sea level is 10 GeV. We assume that the primary photon spectrum can be approximated by a single power-law function

$$J(E_\gamma) = A_\gamma \left(\frac{E_\gamma}{\text{GeV}}\right)^{-\beta}, \tag{10}$$

and only the tail of the GRB photon spectrum would contribute to the muon excess observed on the ground. The photon flux is expressed as $E^2 dN/dE$.

Thus, in the case of the Tupi event 28 September 2011, we obtain the following estimations of the photon flux (at

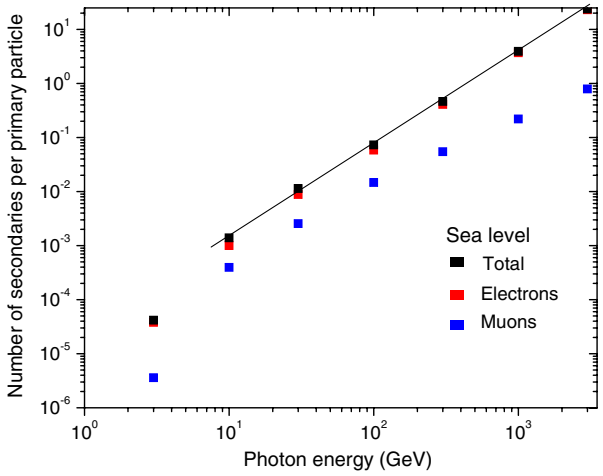

FIG. 19 (color online). The number of charged particles at sea level per photon as a function of incident photon energy from the FLUKA calculations. The line represents a power-law fit for $E_\gamma >$ 10 GeV. The squares correspond to total number of charged particles, electrons, and muons, from top to bottom, respectively.

68% C.L.) in the energy region $E_\gamma \sim 10$ GeV using two choices for the spectral index β: $3.8 \pm 0.8 \times 10^{-6}$erg/cm^{-2} for $\beta = 1.4$ and $1.1 \pm 0.2 \times 10^{-5}$ erg/cm^{-2} for $\beta = 1.5$.

We compare our results with other ground based observation of GRBs in Fig. 20. The Milagrito event (square) has been suggested as the TeV counterpart of the BATSE GRB 970417a [48,49]. For comparison we show the upper limits at 1 and 10 MeV from the EGRET TASC spacecraft detector. The energy spectra for these events and the upper limits of the Tupi event (circles) are also presented in Fig. 20.

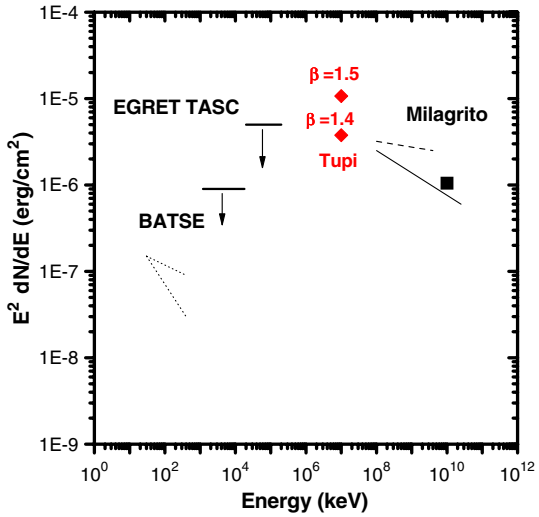

FIG. 20 (color online). Fluence for the Tupi event (circles). For comparison the Milagrito GRB 970417 event (square), upper limits from the EGRET TASC detector (at 1 and 10 MeV), power-law fits to BATSE data, and power-law fits consistent with the Milagrito observations [49] are shown.

VII. CONCLUSION

It is very well known that the primary charged particles come deep down into the atmosphere owing to the low field intensity over the SAA. Consequently, cosmic ray fluxes at low energies in the SAA region are even higher than world averages at comparable altitudes. This situation is reflected as an excess in the counting rate of the primary cosmic rays. Probably this behavior is responsible for the observation of muon excess in association with high energy particles (protons and ions) emitted by flares of small scale, as has been reported by the Tupi experiment.

The flux of particles at ground ($E > 100$ MeV) is not constant, because they are subject to temporal variations due to local weather conditions and they are modulated by solar activity and fluctuations of interplanetary magnetic field. We have presented in this survey a search for a simultaneous signal of solar transient events of small scale in the PAO SD and the Tupi muon telescopes. Both experiments are situated within the SAA area. Of several candidates that were found we presented two events associated with solar flares and two events associated with interplanetary shocks (CIR). Based on experimental observation, we estimated the spectra of accelerated protons in the solar flare and compared our results with other measurements.

We also searched for possible coincident counterparts to the GRB signals in the narrow field of view of the Tupi muon telescopes and in the large solid angle water-Cherenkov detectors of the PAO SD. We found a candidate event with features of likely association with the gamma-ray burst GRB 110928B observed by Swift satellite. The light curve, including background duration and rate significance, is not determined. However, the GRB has an image significance 7.79σ and a trigger with duration of 17.1 min [42]. In addition, the burst location was close to the MAXI source J1836-194.

The GRB observation in the limit of the effective field of view of the vertical Tupi telescope consists of an excess of muons with high signal significance in the 1-sec binning counting rate of muons (raw data) in close time coincidence (T-184 sec) with the Swift-BAT GRB 110928B trigger (trigger = 504307). We found that the probability for such an excess being due to a background fluctuation is $\sim 1.15 \times 10^{-6}$ for 24 h. Following this analysis, we checked whether there were other possible excesses in the vertical Tupi telescope corresponding to the GRB trigger time reported by the satellites. We found that 18 GRBs are compatible with the fluctuations in the background during a ± 500 s period around the trigger time. No other significant correlations were detected comparable with the Tupi 28 September 2011 event. The observation of GRBs at ground level depends on the spectral index value, the highest photon energies of the spectrum, and the burst features. If the excess observed on 28 September 2011 is not a fluctuation of the background, then the energy spectrum of gamma rays from GRB110928B with the power index $\beta < 1.8$ may have been observed. A search for other coincidences with GRB satellite observations, to verify this result, will be continued with the current as well as upgraded detectors within the Tupi project.

ACKNOWLEDGMENTS

This work is supported by the National Council for Research (CNPq) of Brazil, under Grants No. 306605/2009-0 and No. 01300.077189/2008-6, and Fundação de Amparo a Pesquisa do Estado do Rio de Janeiro (FAPERJ), under Grants No. 08458.009577/2011-81 and No. E-26/101.649/2011. We thank the Pierre Auger Observatory for their open data policy making their data freely available through their Web site. We also express gratitude to the ACE/MAG instrument team, the ACE Science Center, and the NOAA Space Weather Prediction Center for valuable information and data used in this study. We express our thanks to the GRB groups of Swift, Fermi, and Konus-Wind for providing online GRB data. The authors wish to thank the anonymous referees for advice, valuable suggestions, and comments.

[1] C. E. Navia, C. R. A. Augusto, M. B. Robba, M. Malheiro, and H. Shigueoka, Astrophys. J. **621**, 1137 (2005).
[2] C. R. A. Augusto, C. E. Navia, and M. B. Robba, Phys. Rev. D **71**, 103011 (2005).
[3] C. R. A. Augusto, C. E. Navia, H. Shigueoka, K. H. Tsui, and A. C. Fauth, Phys. Rev. D **84**, 042002 (2011).
[4] C. E. Barton, J. Geomagn. Geoelectr. **49**, 123 (1997).
[5] C. Boatella, G. Hubert, R. Ecoffet, and S. Duzellier, IEEE Trans. Nucl. Sci. **57**, 2000 (2010).
[6] M. Casolino *et al.* (PAMELA Collaboration), in *Proceedings of the 30th International Cosmic Ray Conference, Mexico City, 2007*, edited by R. Caballero *et al.* (Universidad Nacional Autonoma de Mexico, Mexico City, 2008), Vol. 1, pp. 709–712 [http://indico.nucleares.unam.mx/contributionDisplay.py?contribId=503&confId=4].
[7] J. Abraham *et al.* (Pierre Auger Collaboration), Phys. Lett. B **685**, 239 (2010).
[8] J. Abraham *et al.* (Pierre Auger Collaboration), Phys. Rev. Lett. **104**, 091101 (2010).
[9] H. Asorey (for the Pierre Auger Collaboration), *Proceedings of the 31st International Cosmic Ray Conference (ICRC 2009), Lodz, Poland, 2009*, edited by J. Szabelski and M. Giller (University of Lodz, Lodz, 2010) [http://icrc2009.uni.lodz.pl/proc/pdf/icrc0041.pdf].

[10] C. R. A. Augusto, C. E. Navia, K. H. Tsui, H. Shigueoka, P. Miranda, R. Tocina, A. Velarde, and O. Saavedra, Astropart. Phys. **34**, 40 (2010).
[11] K. Watanabe *et al.*, Astrophys. J. **592**, 590 (2003).
[12] I. Allekotte *et al.* (Pierre Auger Collaboration), Nucl. Instrum. Methods Phys. Res., Sect. A **586**, 409 (2008).
[13] P. Abreu *et al.* (Pierre Auger Collaboration), JINST **6**, P01003 (2011).
[14] http://auger.colostate.edu/ED/scaler.php.
[15] C. R. A. Augusto, A. C. Fauth, C. E. Navia, H. Shigeouka, and K. H. Tsui, Exp. Astron. **31**, 177 (2011).
[16] H. Sasaki, K. Ito, M. Kusunose, T. Horiki, T. Nakatsuka, S. Kino, and Y. Hatano, Nucl. Instrum. Methods Phys. Res., Sect. A **321**, 180 (1992).
[17] Y. Yamashina, T. Yamashina, H. Taira, and H. K. M. Tanaka, Earth Planets Space **62**, 173 (2010).
[18] The scintillating medium is an organic plastic scintillator (a polystyrene solvent with para-terphenyl [C18H14] (1%) and POPOP [C24H16N2O2] (0.03%); CI Industry Co. Ltd).
[19] In the case of electrons the energy losses by bremsstrahlung become dominant above a few tens of MeV and are nearly independent from energy. For electrons 100–1000 MeV the energy loss can be expressed as following $-\Delta E/\Delta X \sim 0.15(\mathrm{g/cm^2})^{-1} \times E(\mathrm{MeV})$. The electron's energy is quickly decreasing via bremsstrahlung, and for energies below the critical value (~ 20 MeV) the ionization process becomes more important and they are absorbed by the flagstones.
[20] In a way, this directionality (narrow angle) of the Tupi telescopes also reduces fluctuations from large angles.
[21] K. Sakura1, Planet. Space Sci. **21**, 793 (1973).
[22] R. J. Murphy and R. Ramaty, Adv. Space Res. **4**, 127 (1984).
[23] J. Poirier, S. Roesler, and A. Fasso, Astropart. Phys. **17**, 441 (2002).
[24] A. Fasso and J. Poirier, Phys. Rev. D **63**, 036002 (2000).
[25] J. Poirier and C. D. Andrea, J. Geophys. Res. **107**, 1376 (2002).
[26] M. Honda, T. Kajita, K. Kasahara, and S. Midorikawa, Phys. Rev. D **70**, 043008 (2004).
[27] R. Abbasi *et al.*, Astrophys. J., **689**, L65 (2008).
[28] W. Q. Gan, Astrophys. J. **496**, 992 (1998).
[29] P. Achard *et al.* (L3 Collaboration), Astron. Astrophys. **456**, 351 (2006).
[30] N. Gopalswamy, M. Shimojo, W. Lu, S. Yashiro, K. Shibasaki, and R. A. Howard, Astrophys. J. **586**, 562 (2003).
[31] H. V. Cane, Space Sci. Rev. **93**, 55 (2000).
[32] B. Heber, T. R. Sanderson, and M. Zhang, Adv. Space Res. **23**, 567 (1999).
[33] D. Eichler, M. Livio, T. Piran, and D. N. Schramm, Nature (London) **340**, 126 (1989).
[34] D. H. Hartmann and S. E. Woosley, Adv. Space Res. **15**, 143 (1995).
[35] A. I. MacFadyen and S. E. Woosley, Astrophys. J. **524**, 262 (1999).
[36] http://gcn.gsfc.nasa.gov/burst_info.html.
[37] X. Bertou *et al.* (Pierre Auger Collaboration), in *Proceedings of the 30th International Cosmic Ray Conference, Mexico City, 2007*, edited by R. Caballero *et al.* (Ref. [6]), Vol. 4, pp. 441–444, (HE part 1) [http://indico.nucleares.unam.mx/contributionDisplay.py?contribId=1042&confId=4].
[38] D. Allard *et al.* (LAGO Collaboration), Nucl. Instrum. Methods Phys. Res., Sect. A **595**, 70 (2008).
[39] C. R. A. Augusto, C. E. Navia, M. B. Robba, and K. Tsui, Phys. Rev. D **78**, 122001 (2008).
[40] http://gcn.gsfc.nasa.gov/gcn3/9009.gcn3.
[41] C. R. A. Augusto *et al.*, arXiv:1109.5156v2.
[42] http://gcn.gsfc.nasa.gov/other/504307.swift.
[43] http://www.astronomerstelegram.org/?read=36 11.
[44] http://www.astronomerstelegram.org/?read=36 89.
[45] Recently, we found that this event being classified as GRB by [42] was not included in the Swift-XRT products for GRBs, http://www.swift.ac.uk/xrt_products/index.php.
[46] A few weeks during this period the Tupi telescopes did not operate due to maintenance or power outage.
[47] A. Fasso, A. Ferrari, J. Ranft, and P. R. Sala, in *Proceedings of the International Conference on Calorimetry in High Energy Physics, La Biodola, Italy, 1993*, edited by A. Menzione and A. Scribano (World Scientific, Singapore, 1993), pp. 493–502.
[48] A. Atkins *et al.*, Astrophys. J. **533**, L119 (2000).
[49] A. Atkins *et al.*, Astrophys. J. **583**, 824 (2003).
[50] http://gcn.gsfc.nasa.gov/konus_grbs.html
[51] http://www.swift.ac.uk/xrt_spectra/00440606/.
[52] http://heasarc.gsfc.nasa.gov/cgi-bin//W3Browse/w3table.pl?Action=Detailed%20Mission&Observatory=fermi